Tony Cho, Youngjae Yu, Seokmin Shin.

Disaggregation Simulation Analysis on Distinct Aβ$_{40}$ Fibril Models

Tony Cho, Youngjae Yu, Seokmin Shin

School of Chemistry, Seoul National University, Seoul 151-747, Korea
Received: March 2, 2016; Accepted: March 22, 2016

Abstract: Aβ$_{40}$ peptides form oligomers that later aggregate into a plaque, which is deemed to be a leading cause of Alzheimer's Disease. Its non-crystalline morphology has limited an understanding of comprehensive structural study. In this research, computational biomolecular simulations were performed in the following order: solvent and ion addition in a box, energy minimization of protein, equilibration, and periodic boundary condition disaggregation of a monomer from fibril. The result founded the two-fold model is 25% more stable in the simulation environment, and the steric zippers held on most tightly until 220 ps of simulation. The study supports the previous findings that two-fold aggregate Aβ$_{40}$ is more stable at 310 K and discusses further how much contribution steric-zipper and hydrogen bonding are making.

Key Words: beta-amyloid, Aβ$_{40}$, steric zipper, simulation

Introduction

Thought to be the cause of Alzheimer's Disease, Aβ$_{40}$ has been clinically tested to be present in 90% of Alzheimer's patients along with two other proteins, CSF Tau protein and P-Tau$_{181p}$. These three comprises good biomarkers of Alzheimer's disease.[1] Previous imaging of Aβ$_{40}$ revealed that it comprises β-sheets running through the entire length of the needle crystals.[2] β-strands within each sheet are *in-register*, which indicates the aligned and ordered stacking of β-sheets. Confirmed by ssNMR, *in-register* β-strands are topologically capable of additional hydrophobic and van der Waals interactions with the identical side chains above and below β-sheets. These interactions appear as interdigitations of side chains like meshing teeth in between stacked β-sheets, so the motif was coined the term, steric-zipper.[2] Steric zippers are stabilized by several factors, including the interdigitation of their two component sheets, their dry interfaces giving hydrophobic stabilization, their tightly fitting interfaces providing van der Waals stabilization, and their stacks of mutually polarizing hydrogen bonds, giving electrostatic stabilization.

A cross-β motif is infinitely extending β-sheets where the β-strands are stacked perpendicular to the long axis of the protofilaments. The steric-zipper interaction and the cross-β spine motif are regarded as the main components in the formation of amyloid state.[3]

Eight distinct classes of Steric-zipper-containing-segments exist that contains different amino acid sequences. Aβ$_{40}$ sequence contains two distinct classes of steric zippers, Class 2-AIIGLM and Class 4-GGVVIA.[4] Steric-zipper-containing-segments, about 7 sequences long, are omnipresent in many types of proteins, yet a few proteins resist forming amyloid. For example, RNase A has several steric-zipper-containing-sequences. When it is denatured, unlike many other proteins, RNase A does not form an amyloid-forming proteins due to a capability known as self-chaperoning.[2]

Numerous work has been conducted on Aβ$_{40}$; however, disaggregation simulation due to its wide variability hasn't been performed. Jang's work on the temperature-dependent populations of various conformers such as trimeric, dimeric, and monomeric mixtures of tetramer simulations have been conducted.[5] The distribution of the oligomeric mixtures as a function of temperatures demonstrates that the dimeric model of Aβ$_{40}$ is most favored at 310 K. The work of disaggregation simulation supports the finding by Nguyen *et. al* that oligomerization is proceeded by two stages: the approach of monomers to the existing oligomer with a rapid increase of β-strand content, and slow rearrangement of both monomer and oligomer into an *in-register* antiparallel form.[6]

Aβ$_{40}$ structures have been suggested as models primarily from Tycko in addition to various Aβ fibril morphologies suggested by ssNMR and cross-β structural motif X-ray fiber diffraction analysis.[7] Moreover, intra-monomeric interaction, β1-β2, is what keeps the monomer contain two β-strands and a β-turn. The polymorphism that arises in a single monomer is called single-chain registration polymorphism.[2] The polymorphism of one monomer unit, or chain, arises often and results into two types of other steric zippers. However, ssNMR structural studies on uniformly isotope-labeled Aβ assemblies have been limited due to Amyloid fibrils are noncrystalline solid materials and incompatible with x-ray crystallography or liquid state NMR and low spectral resolution.[8] Moreover, other molecular-level structural features of amyloid fibrils are not thoroughly established. The lack of comprehensive understanding in structural and molecular characteristics of Aβ$_{40}$ hinders further research on the development of amyloid state inhibitors and disaggregation catalyst. Biomolecular modeling and simulation of proteins and oligomers like Aβ$_{40}$ may

accelerate the understanding of mechanisms and development of the inhibitors.

In this work, two separate models, two-fold and three-fold from Tycko's work, were used in disaggregation simulation at 310 K.[7,9] The pulling simulation involved a pulling of a monomer chain from four layers of β-strands comprising $A\beta_{40}$ fibril.

Theory and Computational Methods

Two models of $A\beta_{40}$ fibrils (PDB code 2LMN and 2LMP), which were suggested by Tycko,[7] were chosen for this work. These two models shared similar β-strand-turn-β-strand topology with -2 side group charged per monomer and a salt-bridge near β-turn, but were different in inter-protofilaments contacts, where I31, G33, M35, and G37 were involved in 2LMN, and where I31, M35, and V39 were involved in 2LMP. In terms of symmetry, 2LMN possessed two-fold symmetry about the fibril growth axis, while 2LMP had three-fold symmetry. Residues 1 to 8 were omitted due structurally disorder in both models. In this work, each fibrillar unit consisted of 4 chains. Chains were labeled sequentially as B, C, D, E, H, I, J, and K in 2LMN, and as B, C, D, E, H, I, J, K, N, O, P, and Q in 2LMP (Figure 1 and Figure 2).

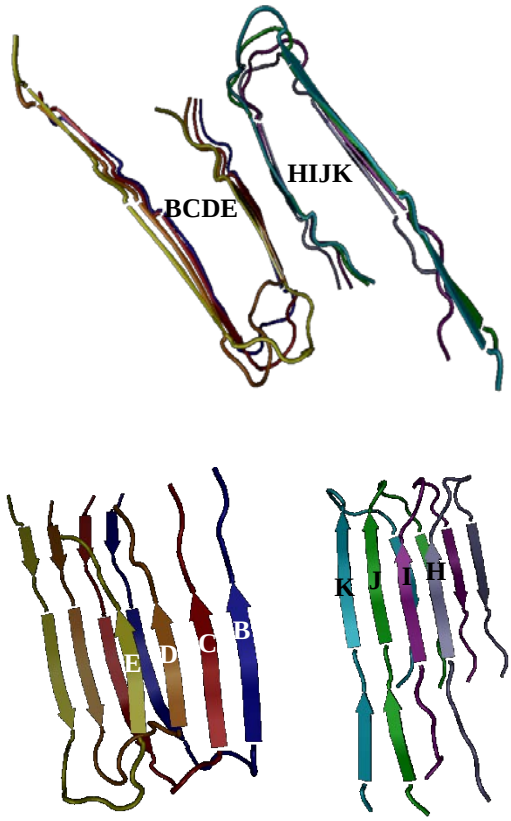

Figure 1. $A\beta_{40}$ two-fold models for a total of eight monomers. A monomer has β-strand, β-turn, followed by β-strand morphology.

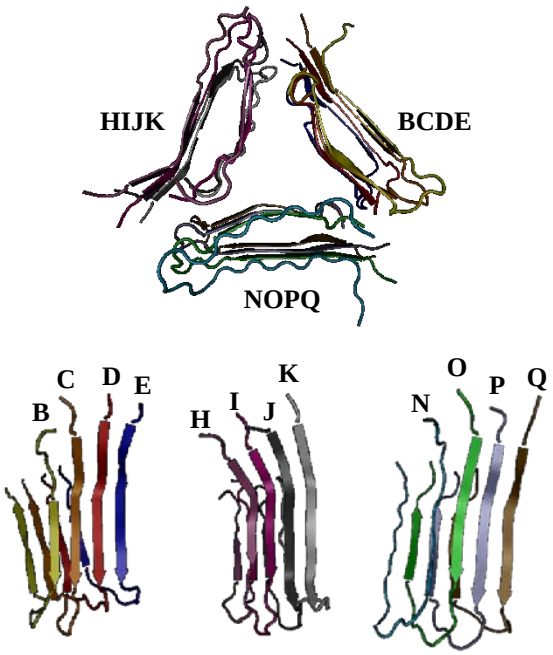

Figure 2. $A\beta_{40}$ three-fold model suggested by Tycko for a total of 12 monomers with three protofibrils held on by interactions

All MD simulations were conducted on GROMACS 5.1 with CHARMM22/CMAP all-atom force field. To prepare initial structures for the pulling simulations, each fibril model was put in a rectangular box of TIP3P water.[10] Z-axis was set as a reaction coordinate, which agrees with the Aβ protofibril growth axis. Considering that the simulation is performed under periodic boundary condition (PBC), the rectangular box whose length in z-axis is long enough was utilized as in Figure 3. 150 mM NaCl was added, including neutralizing counterions. Steepest descents energy minimization was simulated for 100 ps, followed by heating simulation with position restraint on the protein for 3.1 ns. When temperature of the system reached 310 K, position-restrained equilibration was simulated for 5 ns. Force constants for position restraints were 800 kJ/mol/nm^2. Temperature of the system was coupled using Bussi thermostat. Pressure was maintained isotropically at 1.0 bar using Berendsen barostat. Cut-off distances of the Coulomb, the Van der Waals, and the short-range neighbor list interactions were 1.0 nm. Electrostatics was calculated using the particle-mesh Ewald (PME) algorithm.

Tony Cho, Youngjae Yu, Seokmin Shin.

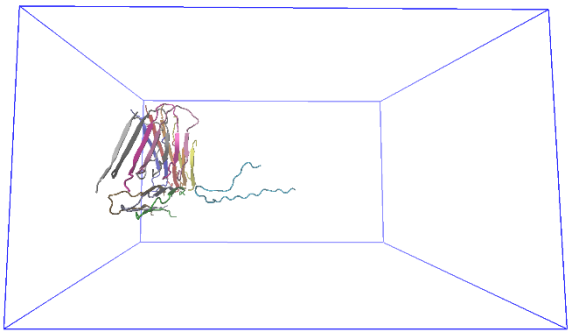

Figure 3. An image of a rectangular box where the PBC disaggregation simulation takes place. Cyan strand (Chain N) was pulled to the right 1Å per ps in the three-fold model.

Following the equilibration, pulling simulations were conducted for 600 ps. Pulling simulations were conducted along a reaction coordinate, or z-axis. The parameters related with interactions were set equally as the equilibration step. Nose-Hoover thermostat and Parrinello-Rahman isotropically-coupled barostat were used with each maintained at 310 K and 1.0 bar. All chains except the end chain (chain K for 2LMN, and chain N for 2LMP) were position-restrained with force constants of 800 kJ/mol/nm^2, and COM of the end chain was pulled along a reaction coordinate using harmonic biasing potential with force constant of 1000 kJ/mol/nm^2. Only z-components of coordinates contributed to the distance, and initial COM distance was set to the starting conformation. The pull rate was 0.01 nm/ps throughout the simulation.

The analysis tools available in GROMACS and VMD were used to analyze the simulations. Distances between residues involved in key contacts were calculated in VMD. The number of hydrogen bonds between the last two chains including the end chain, force, COM position of the end chain, solvent accessible surface area (SASA) were calculated using tools provided in GROMACS. Secondary structure analysis was conducted using DSSP. All molecular graphical presentations were generated by VMD.

Results and Discussions

For the purpose of investigating the distinct features of two-fold and three-fold models of Aβ40, steered molecular dynamics simulation pulling a monomer of $A\beta_{40}$ was performed. Previous work reported that for dimeric, trimeric and tetrameric oligomers were all composed of each Aβ40 monomer made up of two β-strands: β1-strand with residues 10-22 and β2-strand with residues 30-40 residues connected by a bend, or so-called a U-shaped monomer.[5] These two β-strands were held together by interdigitating patterns of amino acid side groups produced by hydrophobic interaction.

β-sheet Structural Characterization

Figure 4 depicts the time profiles of β-sheet structure characterization obtained from Define Secondary Structure of Proteins (DSSP) of two-fold structures and three-fold structure at the normal human body temperature (310 K). According to Figure 4a, two red bands on chain K (top) of graph demonstrate that hydrogen bonds in secondary structure of the two-fold $A\beta_{40}$ are relatively stable until 130 ps and mostly broken by 180 ps. Two red bands on chain N of Figure 4b show that hydrogen bond breaking event of three-fold is initiated at 120 ps and is completed by 220ps. In Figure 4a, the second red band from the top, representing the pulled monomer, β1-strand of Chain K, shrunk in both directions as the band moved to the right. This double-sided shrinkage of a band illustrated that hydrogen bonds in the β1-strand were broken double-sided starting from both residue 10 and residue 22 to residue 16. On the other hand, the top red band, representing β2-strand of Chain K, only shrunk in a single direction. The single-sided shrinkage illustrated that hydrogen bonds were broken single-sided from residue 30 to residue 40.

According to Figure 4a, hydrogen bonds in β2-strand, shown in top band, were broken by 185 ps, and hydrogen bonds in β1-strand was broken by 200ps. While β1-strand was consist of 12 residues, β2-strand was consist of 10 residues. Additional two residues in β1-strand delayed the complete breakage of hydrogen bonds for about 15 ps compared to that of β2-strand. In Figure 4 b, the delay between β1-strand and β2-strand of the three-fold was more apparent, as the hydrogen bonds were removed at about 220 ps and 185 ps, respectively. Compared to other interactions later discussed in the paper, the hydrogen bonding is relatively short-ranged.

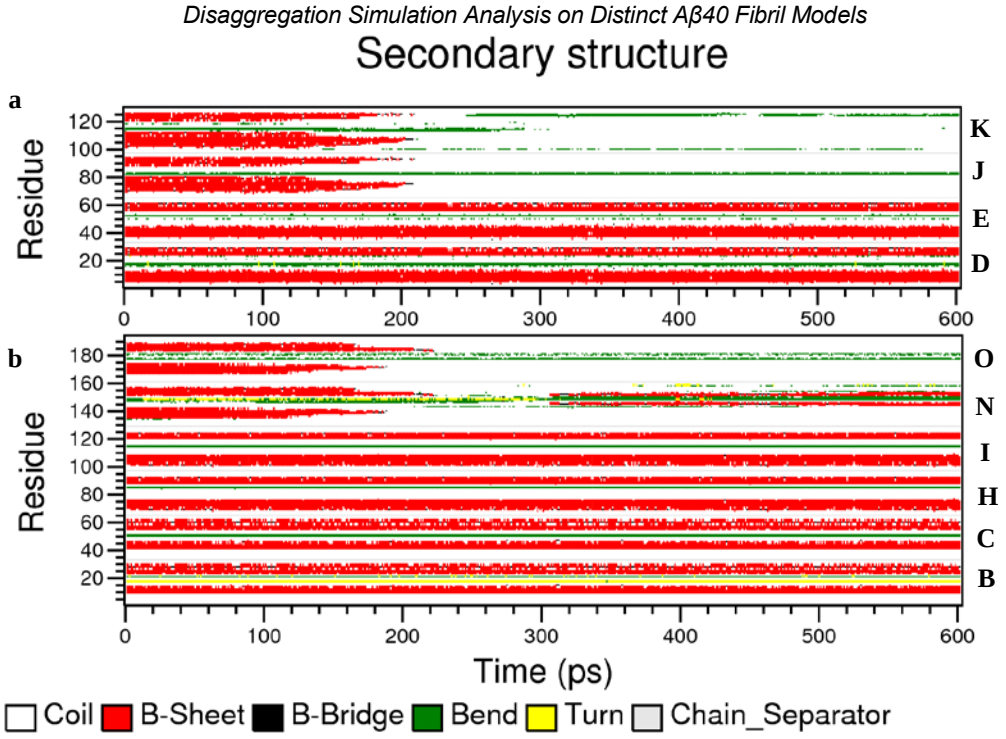

Figure 4. DSSP Analysis of (a) a two-fold model and (b) a three-fold model of a protofillament of $A\beta_{40}$. Each monomer considered were 32 amino acids long. The pulled monomer is represented in residues 97-128 as shown in Figure 4a and is represented in residues 129-160 as shown in Figure 4b.

β2-β2 Inter-protofilaments Steric-Zipper-Forming Segment

Figure 5 shows the distance between residues bound by van der Waals force. The bonds between residues chosen are based on the Tycko's models.[7] In the two-fold model, I31 in the pulled monomer, Chain K, interacts with G37 in the remaining fibril. The intermolecular force is mainly hydrophobic and is quite stable, resisting the pulling until 180 ps, as shown in the blue line in Figure 5a. A similar interaction is observed between G33 in Chain K and M35 in Chain E (green). The next two residues in Chain K are also parts of steric-zipper-forming segments, which are M35 and G37 in Chain K interacting with G33 and I31 in Chain E, respectively. These inter-protofilament contacts were cleaved at 180 ps and 230 ps, indicating more stable hydrophobic force in the region. It may be assumed that the hydrophobic packing regions of G33 and M35 are less accessible by water, so it can be thought these two are more tightly bound. This sequential cleavage trend of β2-β2 steric zippers is also identical to the trend of sequential hydrogen bond breakages in β-sheet, as it was one-sided decay from residue 30. In the three-fold model, the trend shown in Figure 5b follows that I31 (green) in the pulled monomer (Chain N) exhibits the most stable interaction out of all other steric zipper residues. M35 is separated at 180 ps, despite its interaction with two other methionine residues.

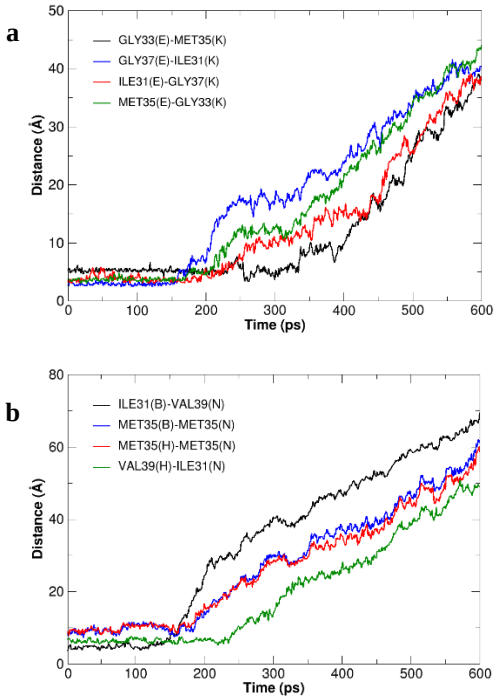

Figure 5. Distance between residues(Å) vs Time(pico-second). Fig 5 (a) shows the two-fold model of $A\beta_{40}$. Fig. 5 (b) shows the three-fold model of $A\beta_{40}$.

Tony Cho, Youngjae Yu, Seokmin Shin.

β1-β2‡ Hydrophobic Interactions*

Among all interactions, β1-β2‡ interactions remained longest. It is shown in Figure 6 that the interaction still existed at 429 ps, apparently long-range interaction. Figure 6 captures a moment in simulation where the pulling of a monomer was momentarily confined from separation by hydrophobic interaction in the pocket. This interaction prolonged immediate separation of the pulled monomers. As shown in Figure 5a, following the separation of inter-filament steric-zipper bond at 220 ps (black), the distance curve plateaus flat, instead of increasing steadily, from 220 ps to about 430 ps, which is an indication for presence of β1-β2‡ interaction. Usually, the VDW force is short-ranged, but this long-range interaction shown by β1-β2‡ seems atypical.[2] Due to the long-range interaction, this result may suggest that the β1-β2‡ interaction allows the formation of cross-β preceding the inter-protofilament steric-zipper β2-β2 contacts in the aggregation of $A\beta_{40}$ because long-range interaction is necessary for quick attraction of $A\beta_{40}$ monomers for statistical favorability during the early stages of $A\beta_{40}$ formation. More favorable, but short-ranged interactions such as hydrogen bonding and β2-β2 interaction could take place afterward. Therefore, this may suggest that elongation of a proto-fibril of $A\beta_{40}$ precedes the formation of inter-protofilament steric-zippers.

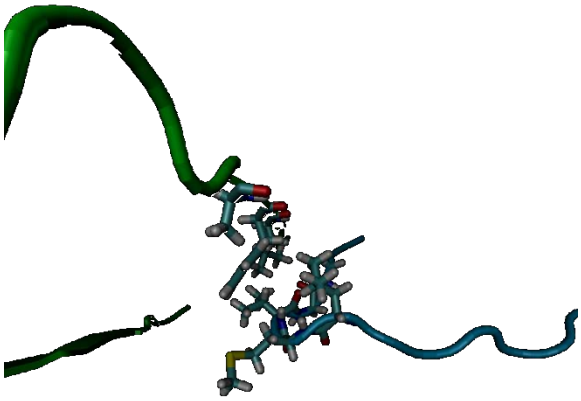

Figure 6. Structure of $A\beta_{40}$ two-fold at 429 ps. The leaving monomer, Chain K, is the chain on the right side (cyan). The chain on its left, Chain J, (green) is from fibril.

Comparison of two-fold and three-fold of $A\beta_{40}$

In Figure 7, the two contrasting force curves and graphical representations of Aβ40 elucidates the difference between the pulled monomers of two-fold and three-fold. From 120 ps to 220 ps, the force curve of two-fold is 10-25% greater than that of three-fold. This difference can be traced to contributions from various intermolecular forces described in the previous figures. Each cross-β unit of two-fold $A\beta_{40}$ contains more number of hydrogen bonds than that of three-fold in average, as represented in Figure 8. At 0 ps, monomer in the two-fold and three-fold makes up 23 and 15 hydrogen bonds, respectively. From 100ps to 150 ps, a monomer of a two-fold makes approximately 15% more than that of a three-fold, while from 150 ps to 200 ps, the difference of hydrogen-bonds enlarges as much as 200% in 165ps. As the number of hydrogen bonds of a monomer in the two-fold and three-fold are approximately similar after 200 ps, the β-sheet contribution in Aβ40 oligomer disaggregation can be neglected after that time. As shown in Figure 9, the amplification of the solvent accessible surface area of β2-β2 interacting residues from 210 ps to 250 ps demonstrates the cleavage of hydrophobic cores during simulation. The β2-β2 interaction in two-folds is maintained mostly by eight residues, while that in three-folds is maintained by nine residues where each chain has three each.

In result, from 280 ps to 320 ps, it is further observed that the two-fold resist pulling disaggregation with approximately 210 kJ/mol/nm while the three-fold resist lightly with less than 140 kJ/mol/nm. The force difference in this region is smaller than that in 100-200 ps range, it suggests that β1-β2‡ interactions only influences the stability of overall Aβ models slightly. This implication is noteworthy in that while the contribution of β1- β2 interaction to the stability of overall amyloid state is minor, steric-zippers and hydrogen bonds are important for the overall stability of amyloid protein.

* β1-β2‡ denotes the interaction between β2-strand of the leaving monomer, and β1-strand of the monomer that is adjacent to the leaving monomer, in parallel direction to β-sheet.

Disaggregation Simulation Analysis on Distinct Aβ40 Fibril Models

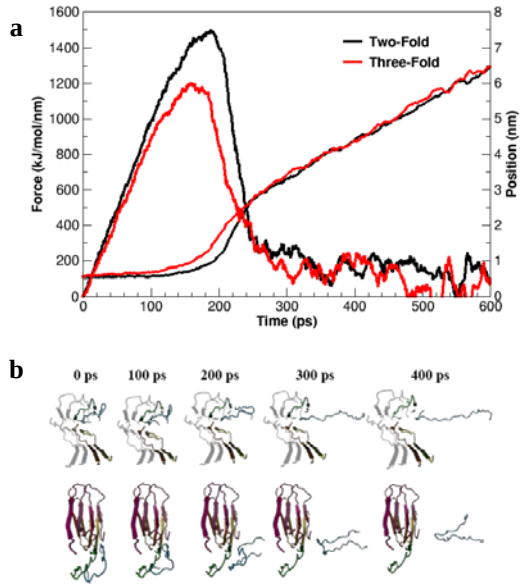

Figure 7. (a) Force curves of two Aβ$_{40}$ models vs time (ps) and distance between the pulled monomer center of mass vs time (ps), (b) graphical representations of two-fold (top) and three-fold (bottom).

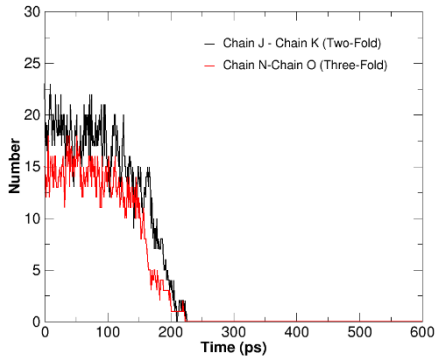

Figure 8. A number of hydrogen bonds formed by β-strands per monomer of Aβ$_{40}$ in two models vs time-frame(ps)

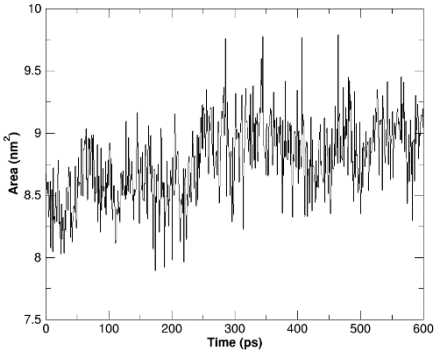

Figure 9. Solvent-Accessible-Surface-Area(SASA) of two-fold model in steric-zipper-forming segment amino acid residues 31, 33, 35, 37 in Aβ$_{40}$ vs time-frame(ps)

Conclusion

The simulation and computation allowed the measurement of properties of Aβ$_{40}$ models where the physical measurement was not yet available for Aβ$_{40}$ and did not promise an accurate result. The force curves of two simulated models, Figure 8, incorporated from the work of Tycko demonstrated when certain interaction dominantly contributed to the pulling resistance. Based on Figure 6, β1-β2‡ interaction remained for the longest time for beyond 250 ps up to 429 ps, which meant the COM was away from adjacent chain by 25-42.9 Å, but the force curve pointed that the difference contributed minimally to the overall stability of Aβ$_{40}$ models. More significant contributions to the stability of amyloid aggregate resulted from the inter-protofilament steric-zipper and backbone hydrogen bonding. This result suggested that an elongated Aβ$_{40}$ proto-fibril that only contained β1-β2‡ interactions and backbone hydrogen bonding were not stable. Therefore, the formation of Aβ$_{40}$ required steric zippers by the structured aggregation of multiple proto-fibrils, instead of a single elongated protofibril. For the further study, Replica-Exchange-Molecular-Dynamics(REMD) simulation of these models may suggest which model was most stable near 310 K, more likely to be primary conformer, and more prone to polymorphisms. Additional research that will be beneficial in the future analysis could include more disaggregation simulations performed at variable temperature, various trajectories, and more complex system to deduce more comprehensively about early formation of amyloid, β1-β2‡ hydrophobic interaction and steric-zippers contributions.

Acknowledgements. This work has been supported by the project EDISON(Education-research Integration through Simulation On the Net), Chemistry.

Reference

[1] Meyer, D. G.; Shapiro, F.; Vanderstichele, H. *Archives of Neurology*. **67**, *8*, 949-956

[2] Otzen, D. E., Ed. *Amyloid Fibrils and Prefibrillar Aggregates: Molecular and Biological Properties*; Wiley-VCH: Weinheim, Germany, 2013.

[3] Goldschmidt, L.; Teng, P. K.; Riek, R.; Eisenberg, D. *Proc. Natl. Acad. Sci. U.S.A.*, **107**, *8*, 3487-3492.

[4] Nelson, R.; Sawaya, M.R.; Balbirnie, M.; Madsen, A. O.; Riekel, C.; Grothe, R.; Eisenberg, D. *Nature*. **435**, *7043*, 773-778.

[5] Jang, S.; Shin, S. Computational Study on the Structural Diversity of Amyloid Beta Peptide ($A\beta_{10-35}$) Oligomers. *J. Phys. Chem. B.* **2008**, *112*, 3479-3484.

[6] Nguyen, P. H.; Li, M. S.; Stock, G.; Straub, J. E.; Thirumalai, D. *Proc. Natl. Acad. Sci. U.S.A.* **2007**, *104*, 111.

[7] Tycko, R. Symmetry-based constant-time homonuclear dipolar recoupling in solid state NMR. *J. Chem. Phys.* **2007**, *126*, 064506-064509.

[8] Bertini, I.; Gonnelli, L.; Luchinat, C.; Mao, J.; Nesi, A. A New Structural Model of $A\beta_{40}$ Fibrils. *J. Am. Chem. Soc.* **2001**, *133*, 16013-16022.

[9] Petkova, A. T., Ishii, Y., Balbach, J.J., Antzutkin, O.N., Leapman, R.D., Delaglio, F., and Tycko, R. *Proc. Natl. Acad. Sci. U.S.A.* **2002**, *99*, 16742.

[10] Lemkul, J. A.; Bevan, D.R. Assessing the Stability of Alzhemier's Amyloid Protofibrils Using Molecular Dynamics. *J. Phys. Chem. B.* **2010**, *114*, 1652-1660.